frontiers | Frontiers in Catalysis

TYPE Original Research
PUBLISHED 03 February 2023
DOI 10.3389/fctls.2022.1096824



OPEN ACCESS

EDITED BY
Karoliina Honkala,
University of Jyväskylä, Finland

REVIEWED BY
Marko Melander,
University of Jyväskylä, Finland
Samira Siahrostami,
University of Calgary, Canada

*CORRESPONDENCE
Younes Abghoui,
younes@hi.is

SPECIALTY SECTION
This article was submitted to Modelling, Theory and Computational Catalysis, a section of the journal Frontiers in Catalysis

RECEIVED 12 November 2022
ACCEPTED 29 December 2022
PUBLISHED 03 February 2023

CITATION
Abghoui Y, Iqbal A and Skúlason E (2023), The role of overlayered nitride electro-materials for $N_2$ reduction to ammonia. *Front. Catal.* 2:1096824. doi: 10.3389/fctls.2022.1096824



# The role of overlayered nitride electro-materials for $N_2$ reduction to ammonia

Younes Abghoui[1]*, Atef Iqbal[1] and Egill Skúlason[1,2]

[1]Science Institute, University of Iceland, Reykjavík, Iceland, [2]Faculty of Industrial Engineering, Mechanical Engineering and Computer Science, University of Iceland, Reykjavík, Iceland

Following our previous report on $N_2$ reduction reaction (NRR) on the surface of nitrides, we investigated the influence of incorporation of titanium nitride as a stable and inactive-NRR material into the structure of DFT-predicted NRR-active surfaces of chromium, vanadium, niobium, and zirconium nitrides. The outcome of our density functional theory (DFT) based analyses suggests that combination of titanium nitride with vanadium nitride can enhance the potential-determining step of the reaction with up to 20% compared to pure vanadium nitride while maintaining similar number of proton-electron transfer steps for formation of two ammonia molecules. The influence of titanium nitride on chromium nitride is expected to be more pronounced as rate-determining step associated with nitrogen adsorption on the vacancy and regeneration of the catalyst improves by around 90% compared to the pure chromium nitride. This effect on niobium and zirconium nitride is, however, negative as the potential-determining step becomes larger for the case of niobium nitride, and the reaction pathway changes from nitrogen reduction to hydrogen evolution for the case of zirconium nitride. These results not only encourage experimentalists to explore these overlayered structures further in experiments, but it also opens up the avenue for considering the alloys and dopants of these nitrides *via* both density functional theory modelling and experiments.

KEYWORDS

**DFT calculations, electrochemical ammonia production, transition metal nitride overlayers, ambient conditions, $N_2$ reduction**

## 1 Introduction

Humanity has accomplished rapid industrial expansion and swift technological advancement in a short period of time since the industrial revolution by utilizing vast quantities of energy resources (Li et al., 2018; Zhou et al., 2022). This promptly expanded the use of fossil fuels as the predominant source of energy to fulfil the enormous energy demand (Hossain and Davies, 2013; Ma et al., 2020). Consequently, contemporary civilization is confronted with resource depletion and terrible environmental problems, such as air pollution and global warming (Holmberg and Erdemir, 2019). In response to this challenge, there is a global campaign toward regularizing utilization of sustainable energy sources for commercial and industrial applications with zero carbon emissions (Pretty, 2013; Loiseau et al., 2016). Ammonia and hydrogen have earned significant interest among the alternatives that could potentially replace fossil fuels due to their abundant reserves and eco-friendliness (Lan et al., 2012). Ammonia's energy density by volume is, however, nearly double that of hydrogen with easier shipment and distribution making it a primary competitor as a green alternative fuel (Giddey et al., 2017). Therefore, it can be applied as a flexible long-term energy storage/carrier means and zero-carbon fuel. For this to be realized, industrial production

of ammonia needs to be transferred from the heavily fossil fuel reliant Haber-Bosch process to a more renewable approach. Electrochemical nitrogen reduction reaction (NRR) to produce ammonia in a renewable manner is one of the most promising approaches and has been the focus of research over the last decade. These works cited here clearly show a summary of the progress in the field, new insights, and current challenges (Cui et al., 2018; Wang et al., 2018; Andersen et al., 2019; Chen et al., 2020; Duan et al., 2020; Gu et al., 2020; Liu et al., 2020; Manjunatha et al., 2020; Qing et al., 2020; Chanda et al., 2021; Choi et al., 2021; Du et al., 2021; Li et al., 2021; Rehman et al., 2021; Shen et al., 2021; Yang et al., 2021; Azofra, 2022; Chen et al., 2022; Fuller et al., 2022; Liao et al., 2022; Zhang et al., 2022)· (MacLaughlin, 2019; Singh et al., 2019; Choi et al., 2020; Dražević and Skúlason, 2020; Hanifpour et al., 2020; MacFarlane et al., 2020; Hanifpour et al., 2022a; Li et al., 2022; Wan et al., 2022; Yao et al., 2022). In catalysis, the utilization of nitrogen-rich transition metals is particularly promising where transition metal nitrides (TMNs) were predicted to be good for making ammonia chemically (Michalsky et al., 2015a; Zeinalipour-Yazdi et al., 2015) and electrochemically (Abghoui et al., 2015; Michalsky et al., 2015b; Abghoui et al., 2016; Abghoui and Skúlason, 2017a; Abghoui, 2017; Abghoui and Skúlason, 2017b; Garden et al., 2018; Gudmundsson et al., 2022) through a Mars-van Krevelen mechanism. We explored a wide range of TMN surfaces *via* density functional theory (DFT) calculations for the possibility of catalyzing NRR where ZrN, VN, CrN, and NbN were nominated as promising material (Abghoui et al., 2015; Abghoui et al., 2016; Abghoui and Skúlason, 2017a; Abghoui and Skúlason, 2017b; Abghoui and Skúlason, 2017c), and TiN along with other earlier TMNs found inactive for NRR (Abghoui and Skúlason, 2017d; Abghoui, 2022), all in the (100) facets of the rocksalt structure. We tested some of these candidates experimentally in our laboratory and agreement was found between our theory and experiment demonstrating stronger nitrogen adsorption for ZrN and NbN and the earliest reaction onset potential for VN (Hanifpour et al., 2022b). The theoretically predicted onset potential values for NRR were found to agree with the experimentally observed ones. Among the four nitrides, however, ZrN was the only nitride that demonstrated stability in both Ar and $N_2$ solutions at the NRR active potentials. However, the surface stability of other TMNs (VN, CrN, and NbN) studied experimentally was found not to be optimal in the operating conditions without which it is not possible to make a fair judgement of their activity and selectivity. This lack of stability can possibly be addressed by increasing access to $N_2$(g) and/or engineering the surface. From both our theoretical and experimental analyses, we know that TiN is not interesting for NRR but it offers electrochemical stability under operating conditions. Also there are several applications for TiN benefitting from its high stability in electrochemistry where for example palladium nanoparticles assembled on TiN enhanced electrochemical reactions in water (Fu et al., 2018) or presence of TiN enabled highly stable lithium-sulfur battery systems (Cui et al., 2016). Thus, the incorporation of an NRR-stable but inactive material like TiN into the structure of an NRR-active but unstable material such as CrN, VN, and NbN might enhance the stability due to synergistic effects and changes in electronic configurations. To investigate this hypothesis, we have modelled these promising TMNs on TiN as substrate. Since it will be experimentally challenging to control the number of overlayers, we investigated different monolayers as one, two, and three overlayers of a given TMN on TiN substrate, the details of which come up in the following sections.

## 2 Methodology

All DFT calculations were performed with the RPBE (Hammer et al., 1999) exchange correlation functional while the core electrons were described by a PAW representation (Blöchl, 1994), and the valence wave functions were expanded in a basis set of plane waves with an energy cutoff of 350 eV. Our test calculations confirm that the effect of employing higher cutoff value (500 eV) is as small as 20–45 meV on adsorption energy of the $N_2$, NH, $NH_2$, and $NH_3$ species on the surface (Abghoui and Skúlason, 2017b). Therefore, 350 eV was chosen as relatively fair compromise between accuracy and computational time. To see the effect of a dispersion corrected functional (Grimme et al., 2010), test calculations conducted for NH, $NH_2$, and $NH_3$ adsorption on the surface and comparison between the RPBE functional and the RPBE-D3 showed less than 0.1 eV difference which is neglected in this work. The occupation of the Kohn–Sham states was smeared according to a Fermi–Dirac distribution with a smearing parameter of kBT = 0.1 eV. Activation energies were calculated as the highest point along the minimum energy path (MEP) acquired using the climbing image nudged elastic band method (CI-NEB) developed by Henkelman and Jónsson (2000). A 4 × 4 × 1 Monkhorst–Pack k-point sampling is used for all the surfaces. For band structures and DOS calculations, the Brillouin zone was also sampled with 6 × 6 × 1 and 12 × 12 × 1 k-grid meshes. All calculations were performed using the Vienna *ab initio* simulation package (VASP) (Kresse and Furthmüller, 1996). The electrochemical reactions were modelled as detailed in our previous work (Abghoui et al., 2016). The thermochemical and computational hydrogen electrode model used here shown accurate for NRR on predicting the reaction pathways and onset potentials (Tayyebi et al., 2019; Höskuldsson et al., 2021). The model surface of the nitrides was composed of a five-layer slab containing four atoms of nitrogen and four atoms of the relevant transition metal in each layer. The two bottom layers were fixed while the rest, including any adsorbed species, was allowed to fully relax. The relaxed structure of TiN, with lattice constants of 4.29 Å (Hlynsson et al., 2014), was used as substrate here to model the overlayers. Three different overlayers were studied on TiN, one overlayer of the targeted TMN on four layers of TiN (denoted as 1TMN; like 1CrN), two overlayers of the targeted TMN on three layers of TiN (denoted as 2TMN; like 2CrN), and three overlayers of the targeted TMN on two layers of TiN (denoted as 3TMN; like 3CrN), see Figure 1 for a schematic illustration of the model. Boundary conditions were periodic in the *x* and *y* directions and surfaces were separated by more than 12 Å of vacuum in the *z* direction. The structural optimization was considered converged when the forces in any direction on all moveable atoms were below 0.01 eV·Å$^{-1}$. In this work, the rate-determining step (RDS) is associated with a non-electrochemical step such as $N_2$ adsorption and $NH_3$ desorption where the step cannot be tuned by applying external potential. While the potential-determining step (PDS) is associated with the electrochemical steps such as protonation steps. The largest difference between the two adjacent electrochemical steps is considered to be the PDS.

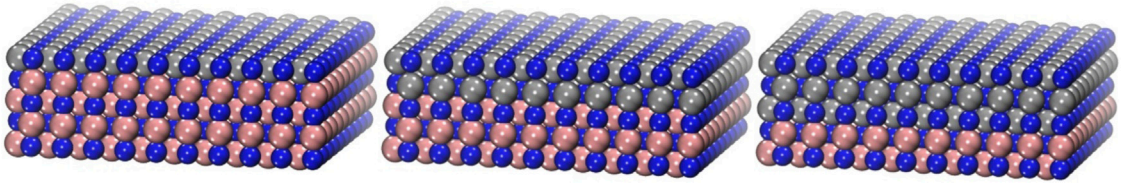

FIGURE 1
Schematic representation of the modelled system for one, two, and three monolayers of CrN on TiN, from left to right respectively, tilted side view. Blue represents nitrogen, grey chromium, and bronze titanium. The unit cell is repeated in the *x* and *y* directions.

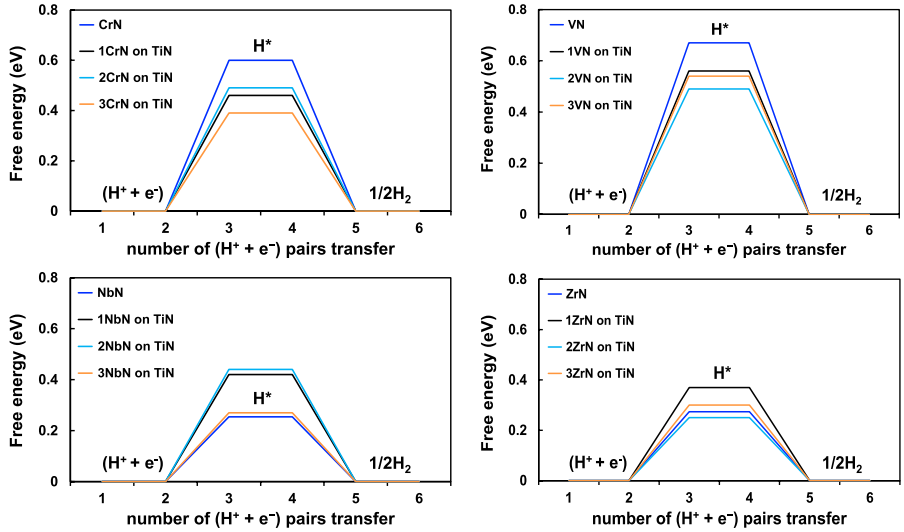


FIGURE 2
H*-descriptor-based free energy diagrams for HER for the four TMN-based overlayered structures.

The operational reaction of the Mars-van Krevelen mechanism toward $NH_3$ formation and nitrogen vacancy creation and its regeneration by $N_2$ molecule is shown below:

$$* + 6(H^+ + e^-) \rightleftharpoons *H + 5(H^+ + e^-) \quad (1)$$

$$*H + 5(H^+ + e^-) \rightleftharpoons *2H + 4(H^+ + e^-) \quad (2)$$

$$*2H + 4(H^+ + e^-) \rightleftharpoons *3H + 3(H^+ + e^-) \quad (3)$$

$$*3H + 3(H^+ + e^-) \rightleftharpoons *^{-N} + NH_{3(g)} + 3(H^+ + e^-) \quad (4)$$

$$*^{-N} + 3(H^+ + e^-) + N_{2(g)} \rightleftharpoons *N_{vac} + *N_{metal} + 3(H^+ + e^-) \quad (5)$$

$$*N_{metal} + 3(H^+ + e^-) \rightleftharpoons *NH + 2(H^+ + e^-) \quad (6)$$

$$*NH + 2(H^+ + e^-) \rightleftharpoons *NH_2 + (H^+ + e^-) \quad (7)$$

$$*NH_2 + (H^+ + e^-) \rightleftharpoons *NH_3 \quad (8)$$

$$*NH_3 \rightleftharpoons * + NH_{3(g)} \quad (9)$$

## 3 Result and discussion

The energetics of all the intermediates along the reaction path to formation of two ammonia molecules have been obtained by doing DFT calculations and investigation of all the possible adsorption sites for each protonation step. As the first step towards hydrogen evolution reaction, the free energy of adsorption of proton on the metal site is obtained and shown in Figure 2. As can be seen, there is no specific trend in the adsorption of proton on these structures and thus these steps should all be well investigated. For both CrN and VN on TiN, proton adsorption on the pure TMN is weaker than on the overlayered structures, which is not the case for NbN and ZrN. However, this step on all these structures is endergonic and this can be an indication of improbability of HER. Proton adsorption on overlayered structures of NbN and ZrN becomes less endergonic might be an indication of more prospect of HER. This will be further investigated when we obtain the free energy diagrams in the upcoming sections as the reaction path towards either $NH_3$ or $H_2$ will be discovered.

Figure 3 shows the free energy diagrams constructed from obtaining the energies of all possible intermediates along the reaction path where TiN was used as sublayers or substrates for these four promising TMN surfaces. The presence of TiN (as a stable TMN under experimental conditions) is expected to show positive effect on overall stability of these material. Considering CrN@TiN, the potential-determining step (PDS; an electrochemical step tunable by applying potential) was found to be improved from 0.41 eV (on pure CrN) to 0.26 eV (on 2CrN@TiN), around 37%

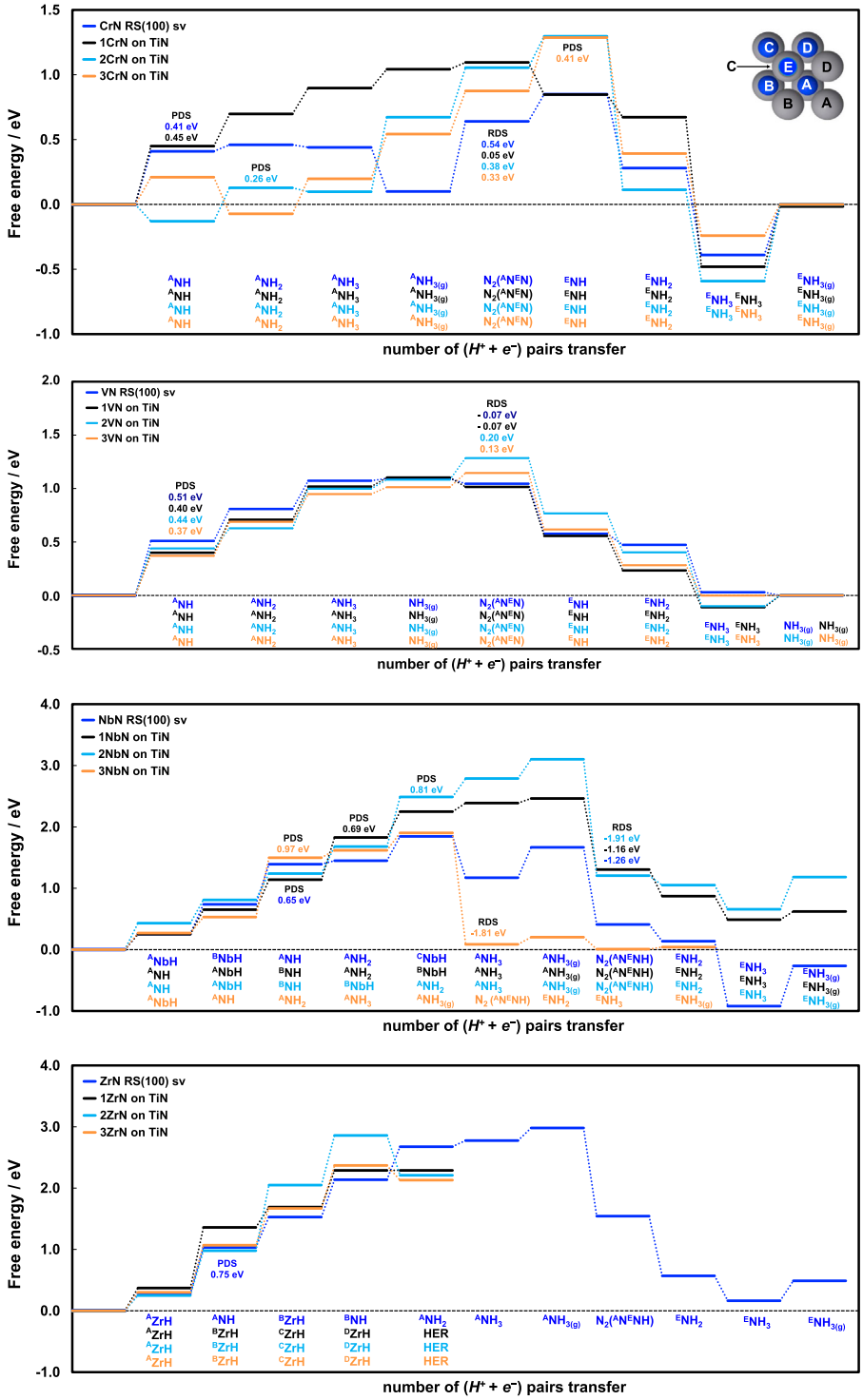


FIGURE 3
Free energy diagrams for CrN, VN, NbN, and ZrN as pure TMN and when combined with the stable TiN as substrate with different number of monolayers.

enhancement in PDS which is corresponding to 37% enhancement to the onset potential (as U = - ΔG). More importantly, the rate-determining step (RDS; non-electrochemical step) associated to dissociation of $N_2$ molecule for regenerating the catalyst (which is a parameter of stability as well) was found to improve for all the chromium-titanium overlayered structures, especially for the first overlayer of chromium on titanium where 0.54 eV (on pure CrN) drops to 0.05 eV (on 1CrN@TiN) facilitating this step at ambient conditions. This is around 90% enhancement on the thermodynamics of the nitrogen adsorption and replenishment of the N-vacancy that should contribute to better stability. Surprisingly, all the reaction steps with regards to proton/electron transfer remain similar to pure CrN predicting that the selectivity should not be compromised with incorporation of TiN. Therefore, the presence of TiN is expected to

10.3389/fctls.2022.1096824

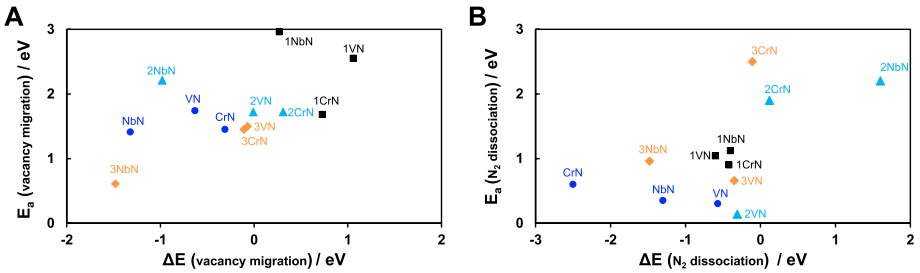


FIGURE 4
**(A)** Energy differences, $\Delta E_{(\text{vacancy migration})}$, of presence of a N-vacancy at the surface layer and in the first subsurface layer of a nitride and the associated activation energy of N-vacancy migration, $E_{a\ (\text{vacancy migration})}$. **(B)** Energy differences, $\Delta E_{(N_2\ \text{dissociation})}$, of nitrogen molecule dissociation on a N-vacancy at the surface layer and the associated activation energy, $E_{a\ (N_2\ \text{dissociation})}$. The larger the $E_a$ is, the slower would be the rate of the reaction according to $k = \nu \exp(-E_a/k_BT)$, where $\nu$ is the normal attempt frequency as the prefactor, $E_a$ is the activation energy (eV) of the reaction, $k_B$ is the Boltzmann constant and T is the temperature. Since ZrN overlayers do not result in ammonia formation, these analyses have not included ZrN overlayers.

enhance the overall performance of CrN as it improves the onset potential of CrN, facilitates nitrogen adsorption to the nitrogen-vacancy, and is expected to improve the catalyst regeneration and catalyst stability while maintaining the same level of selectivity.

For VN@TiN, the PDS improves from 0.51 eV (on pure VN) to 0.37 eV (on 3VN@TiN) indicating of 14 mV better onset potential (~28% enhancement). Comparing pure VN with 1VN@TiN, the onset potential enhances by 11 mV (~22% enhancement), and the associated RDS remains as small as −0.07 eV. Upon introduction of second and third monolayers of VN on TiN the RDS step becomes slightly endergonic. Here also all the steps towards ammonia formation remain similar to that of pure VN, suggesting similar level of selectivity. Therefore, integration of pure VN with TiN is expected to enhance the onset potential and stability while maintaining similar level of selectivity.

The case of NbN and ZrN, however, was found to be different. Such integration with TiN seems negatively affecting the onset potential of NbN as the PDS increases from 0.65 eV on pure NbN to 0.97 eV on 3NbN@TiN. In addition to PDS, the RDS also increases from 1.2 eV to 1.9 eV hardening the thermodynamics of nitrogen dissociation and regeneration of the N-vacancy. For ZrN, inclusion of TiN changes the reaction pathway drastically in a way that unlike pure ZrN that was predicted and later experimentally shown to catalyse NRR, all the ZrN@TiN overlayered structures could result in HER. Half a monolayer of proton ($4H^+$) on all the overlayered structures of ZrN (ZrN@TiN) results in occupying all the metal sites after which any additional protonation on the surface leads to proton recombination and evolution upon structural relaxation, without possibility of NH formation.

As the sustainability of the catalytic cycles in these nitride materials depends on faster vacancy refilling with atmospheric nitrogen rather than nitrogen migration from the bulk of catalyst to its surface, it is necessary to study both the thermodynamics and kinetics of these reactions to understand the stability. Our hypothesis is that the concept of nitride regeneration is linked with nitride stability and if there is no obstacle on nitride regeneration either due to difficult $N_2$ adsorption to the nitrogen vacancies or due to easy migration of bulk nitrogen to the surface, the nitride should regenerate and thus show relatively good stability. The created vacancy on the surface should be regenerated with atmospheric nitrogen faster than subsurface nitrogen migrating to the surface, otherwise all the nitrogen content of the catalyst will be reacted, and the catalyst will decompose to its parental metal. Therefore, in addition to thermodynamics, the activation energies of these two key processes were investigated to obtain a kinetic understanding of these phenomena for all the overlayered structures except for ZrN@TiN as this combination found not interesting for NRR. Both thermodynamics and kinetics results of these important processes are shown in Figure 4, as 1) kinetics of vacancy migration as a function of its thermodynamics, and 2) kinetics of nitrogen dissociation to regenerate the vacancy as a function of its thermodynamics. For all the overlayered structures with negative ΔE, the migration of the sublayer nitrogen to the surface vacancy becomes favourable. However, activation energies above 1.0 eV are indications that such phenomenon is difficult to occur at ambient conditions and thus very slow. The higher the activation energy, the harder and slower will that process be. Among all, 3NbN with negative ΔE values are the only structures with activation energy below 1.0 eV and thus this migration is expected to happen and contribute to catalyst decomposition and instability. For other structures, even if this process can be thermodynamically favourable, very high activation energies are expected to slow it down at ambient conditions and offer better stability. For nitrogen dissociation and regeneration of the vacancy, the negative values of ΔE are indicative of likelihood of nitrogen dissociation and regeneration thermodynamically. For most of the studied structures, the activation energy of nitrogen dissociation is small ($E_a \leq 1.0$ eV). This means that nitrogen dissociation and catalyst regeneration is expected to happen at ambient conditions. Thus, when comparing decomposition with regeneration, the general conclusion is that regeneration is expected to occur more than decomposition for most of these structures, and this should offer a relatively stable structure under operating conditions. Considering the free energy diagrams in Figure 3 and both Figures 4A, B suggests that 1CrN@TiN and 1VN@TiN should be very interesting surfaces for further analyses and experimental tests.

The free energy barriers ($G_a$) for each process are displayed in Figure 5, where for the vacancy migration process $G_a = E_a$ but for the process of replenishing the vacancy $G_a = E_a + 0.6$, which the 0.6 eV is associated to the entropy loss of $N_2$ from gas phase to the adsorbed state taken from ref (Lide, 2004; Abghoui et al., 2016). In Figure 5, the comparison of migration and regeneration for pure TMN comes first to the left (as denoted) and then the first, second, and third overlayers come to the right side of the pure TMN. Considering Figures 4, 5 for CrN@TiN overlayered structures, both the thermodynamics and kinetics are in favour of nitrogen dissociation and regeneration of the vacancy for the 1CrN@TiN structure, and thus a better stability. For 2CrN@TiN, vacancy migration is not favourable thermodynamically with positive ΔE

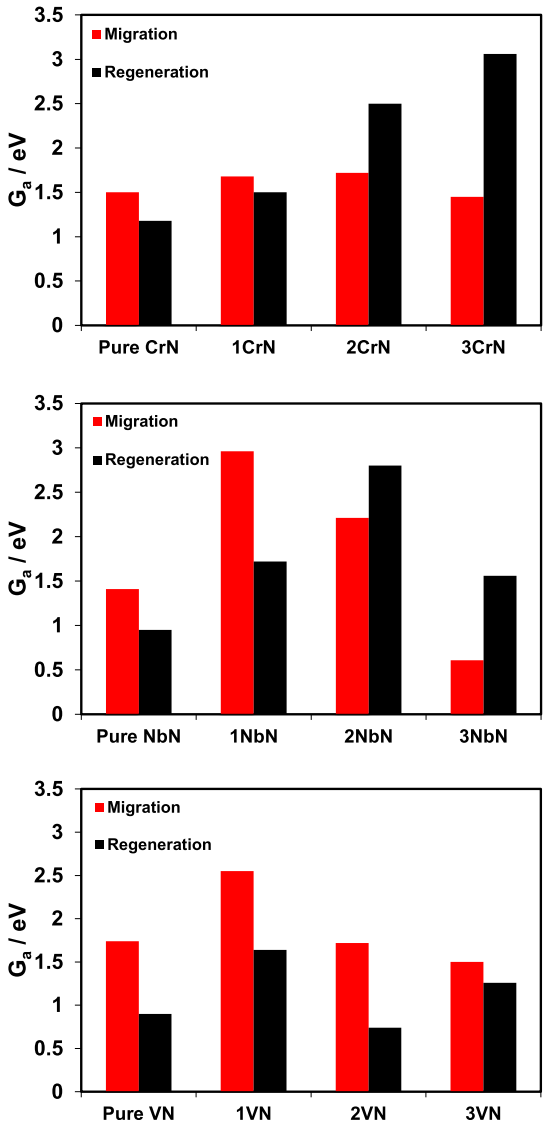


FIGURE 5
The activation free energy of the vacancy migration to the bulk compared with the activation free energy of vacancy refilling. The more positive the value is, the slower would be the rate of the reaction according to $k = \nu \exp(-E_a/k_BT)$. Since ZrN overlayers on TiN do not result in ammonia formation, these analyses have not included ZrN overlayers.

values compared to the pure CrN, but kinetically the $G_a$ for migration is smaller than $G_a$ for regeneration and thus this structure could decompose. The 3CrN@TiN is expected to be unstable where both thermodynamics and kinetics of these processes dictate catalyst decomposition due to much faster migration.

For VN@TiN, all the three overlayered structures are thermodynamically more stable than the pure VN with positive ΔE values of migration. Also kinetically, all the overlayered structures of VN are expected to offer a relatively better stability considering smaller $G_a$ values for regeneration process.

For NbN@TiN overlayered structures, it is only 1NbN@TiN structure for which vacancy is stable on the surface thermodynamically with positive ΔE values and the rest including pure NbN have very negative ΔE values and thus representing unstable vacancy on the surface. With regards to kinetics, 1NbN@TiN also shows the largest difference of $G_a$ between migration and regeneration (more than 1 eV) and thus decomposition for this structure is expected to be a slow process. 2NbN@TiN and 3NbN@TiN are expected to decompose from both the thermodynamics and kinetics point of view. In general, it is important to note here that although the barriers for migration process are found to be higher than the barriers for regeneration process for some of these structures, it does not necessarily mean that the catalyst should be stable because the barriers for the regeneration process should be low enough to occur at ambient conditions, and this will be needed to test in experiments.

After $NH_3$ formation and creation of vacancy on the surface of these material, there is a possibility that this vacant active site will be blocked by other species from the electrolyte such as H*, O*, and OH* under operating potentials. If the adsorption free energy of these species is stronger than adsorption free energy of nitrogen, then the active site will be blocked, and the catalytic cycle will be ceased. For all these surfaces, the adsorption free energies have been calculated and plotted in Figure 6. The negative bars show that nitrogen adsorption should be favoured than absorption of other species under negative potentials. As seen, the chance of poisoning is more for 3VN@TiN by O*, and 3CrN@TiN and 1NbN@TiN by H*, while all the rest are expected to be stable against poisoning under electrochemical conditions.

In general and with consideration of the results presented above, the most promising candidates suggested for experimental tests are CrN@TiN and VN@TiN, while NbN@TiN and ZrN@TiN are not expected to be efficient in these overlayered structures. There is no experimental study on formation of overlayers on nitrides as this is a relatively new idea for NRR. However, there are several studies on other metal-based overlayers and near surface alloys that showed promising result of the use of overlayers due to their synergistic effects and modified electronic configurations for reactions. For example, Kelly and Chen (2012) reviewed metal overlayer on metal carbide substrate as unique bimetallic properties for catalysis and electrocatalysis where supporting a Pt metal monolayer on a carbide substrate exhibit similar catalytic and electrocatalytic activity to the corresponding Pt-based systems while demonstrating the advantages of lower cost and higher stability. Inumaru et al. (1997), also investigated synthesis of vanadium oxide overlayers on $SiO_2$ supports. There is also study on Mo@Pt overlayers that showed efficient catalysis for hydrodeoxygenation of guaiacol and anisole (Lai et al., 2017).

The electronic band structures of these overlayered material and the projected density of states (PDOS) values of one, two, and three monolayers of CrN, NbN, ZrN, and VN over TiN, as well as their state (s, p, d) resolved DOSs are also calculated and shown in Figures 7, 8, respectively. As there are contribution from the conduction band to the valence band on the electronic band structures, all of these overlayered structures represent metallic properties. In the PDOS there is a substantial hybridization between the N states and the metal states, since the energy and form of the partial DOSs for the N and metal atoms are highly similar. As shown in Figure 8 the Fermi level is crossed by d-orbitals of titanium and p-orbitals of nitrogen atoms in one monolayer structure. It is interesting to note that raising the layers above TiN causes the Fermi level to be mostly covered by Cr, Nb, Zr, and V d-orbitals, being more pronounced for Cr and V. This causes the system to have more charge carrier by dopant layers. Consequently, manipulating the doping layers of CrN, NbN, ZrN, and VN might be an efficient method of stabilizing the structure and charge carrier.

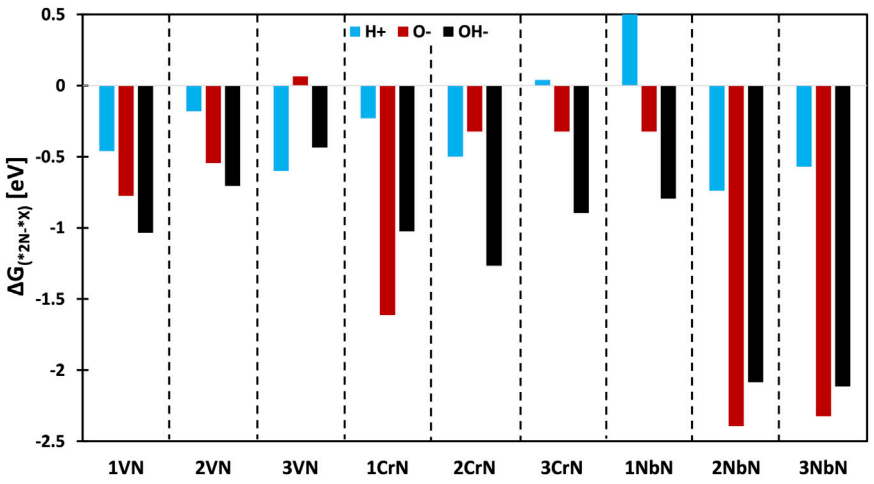


FIGURE 6
The stability against poisoning under electrochemical conditions, the values are obtained at the onset potential needed for initiation of NRR.

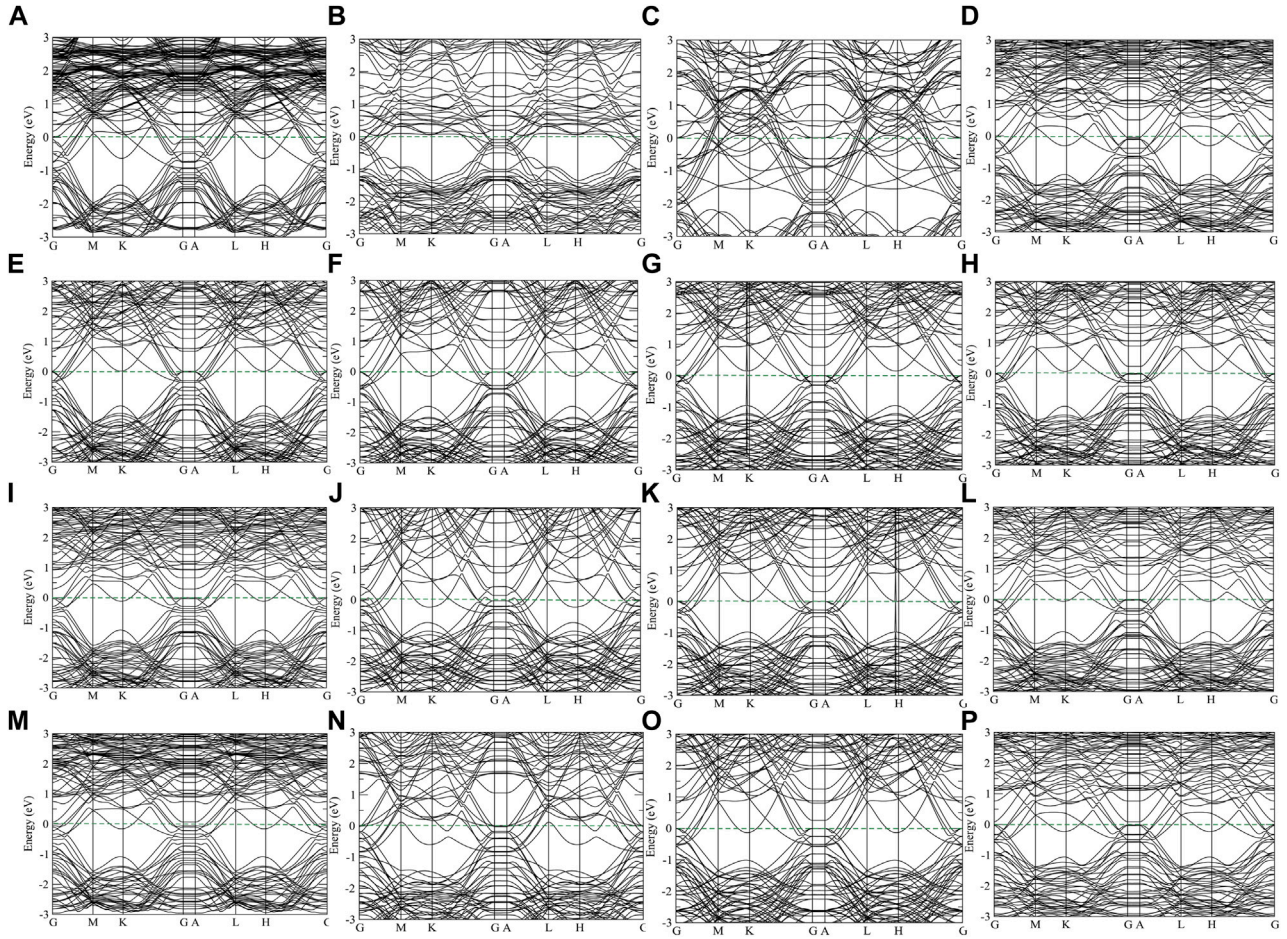


FIGURE 7
The electronic band structures of clean **(A)** CrN, **(B)** NbN, **(C)** ZrN and **(D)** VN, one layer of **(E)** CrN, **(F)** NbN, **(G)** ZrN, and **(H)** VN, two overlayers of **(I)** CrN, **(J)** NbN, **(K)** ZrN, and **(L)** VN, three overlayers of **(M)** CrN, **(N)** NbN, **(O)** ZrN, and **(P)** VN on TiN, respectively. The Fermi energy is set as zero energy point.

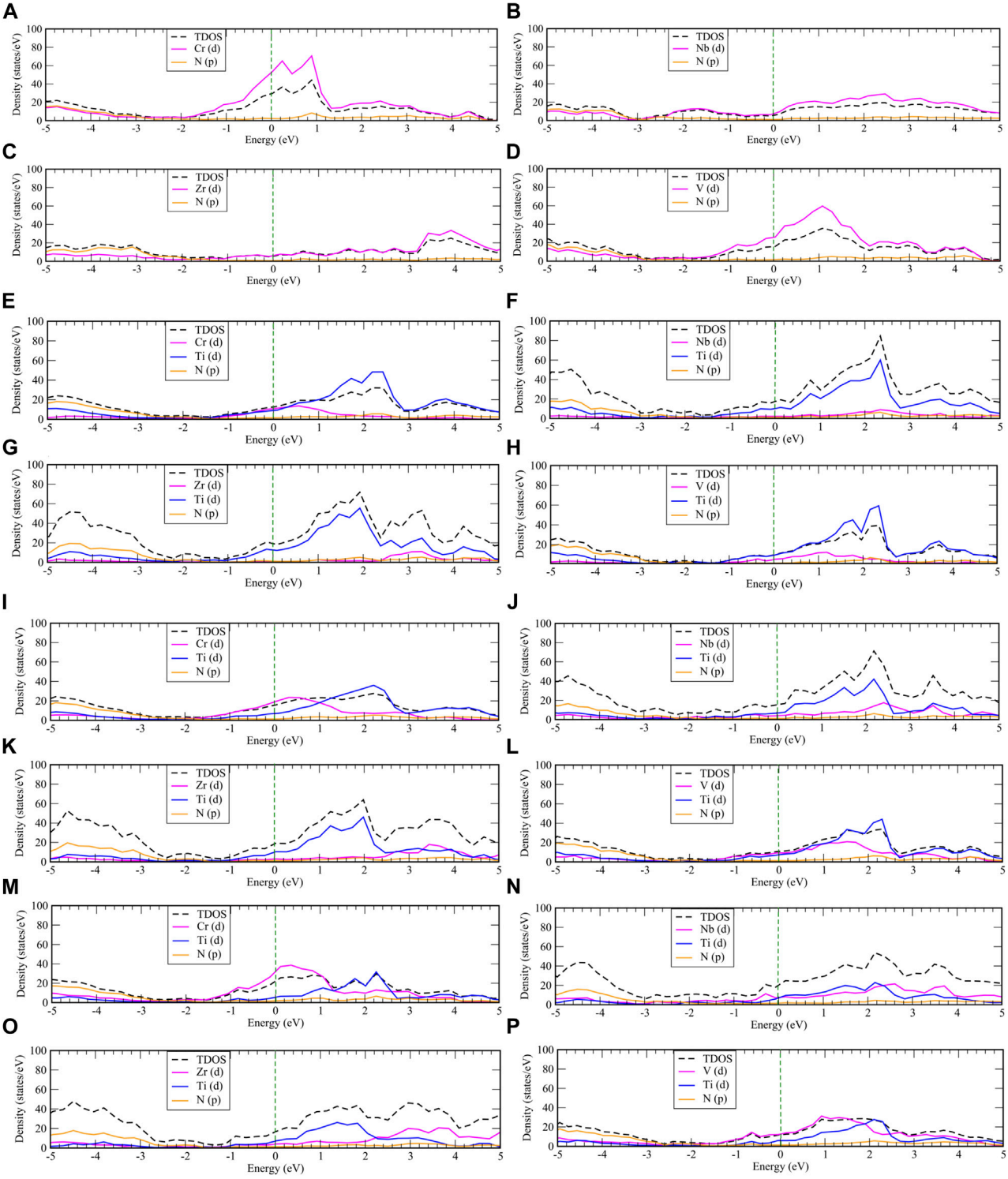


FIGURE 8
The total and partial density of state of pure **(A)** CrN, **(B)** NbN, **(C)** ZrN and **(D)** VN, one overlayer of **(E)** CrN, **(F)** NbN, **(G)** ZrN, and **(H)** VN, two overlayers of **(I)** CrN, **(J)** NbN, **(K)** ZrN, and **(L)** VN, three overlayers of **(M)** CrN, **(N)** NbN, **(O)** ZrN, and **(P)** VN on TiN, respectively. The vertical dashed line indicates the Fermi energy.

## 4 Conclusion

This investigation shows that incorporation of an NRR-inactive TMN such as TiN into an NRR-active TMN such as VN and CrN may enhance the onset potential while pertaining the same mechanism and reaction pathway. This incorporation has also shown to positively impact on free energy of adsorption of $N_2$ specially on CrN where an endothermic bottleneck step like $N_2$ adsorption becomes considerably

less endothermic and more facile and favourable. This overlaying approach, however, was found not promising for NbN and ZrN because presence of TiN decreases the onset potential of NbN by negatively affecting both the PDS and RDS, and completely deactivates ZrN for NRR. The electrochemical stability of TiN is expected to help stabilizing other active nitrides in experiments and this could be opening new avenues for exploring alloys or dopants of these material. Both VN and CrN on TiN are expected to be stable against poisoning and decomposition. With incorporation of TiN, VN is expected to gain more activity and stability. For CrN, the main impact is on lowering the free energy of $N_2$ adsorption and enhancing regeneration of the surface and thus both are interesting for experimental tests.

## Data availability statement

The raw data supporting the conclusion of this article will be made available by the authors, without undue reservation.

## Author contributions

YA conceptualized the project, conducted the modelling and calculations, extracted the data, constructed the figures, wrote the first draft of the manuscript, and provided funding for doing the research. AI performed DOS-related analyses and read the manuscript. ES read the manuscript and commented on it.

## Funding

This work was supported by the Icelandic Research Fund [grant numbers 185051-051, 207056-052, and 196437-051], and the Research Fund of the University of Iceland.

## Conflict of interest

The authors declare that the research was conducted in the absence of any commercial or financial relationships that could be construed as a potential conflict of interest.

## Publisher's note

All claims expressed in this article are solely those of the authors and do not necessarily represent those of their affiliated organizations, or those of the publisher, the editors and the reviewers. Any product that may be evaluated in this article, or claim that may be made by its manufacturer, is not guaranteed or endorsed by the publisher.

## References

Abghoui, Y., Garden, A. L., Hlynsson, V. F., Björgvinsdóttir, S., Ólafsdóttir, H., and Skúlason, E. (2015). Enabling electrochemical reduction of nitrogen to ammonia at ambient conditions through rational catalyst design. *Phys. Chem. Chem. Phys. [Internet]* 17, 4909–4918. doi:10.1039/C4CP04838E

Abghoui, Y., Garden, A. L., Howalt, J. G., Vegge, T., and Skúlason, E. (2016). Electroreduction of N2 to ammonia at ambient conditions on mononitrides of Zr, Nb, Cr, and V: A DFT guide for experiments. *ACS Catal.* 6 (2), 635–646. doi:10.1021/acscatal.5b01918

Abghoui, Y. (2017). *Novel electrocatalysts for sustainable ammonia production at ambient conditions*. Reykjavik: University of Iceland. ISBN: 9789935934420.

Abghoui, Y., and Skúlason, E. (2017). Computational predictions of catalytic activity of zincblende (110) surfaces of metal nitrides for electrochemical ammonia synthesis. *J. Phys. Chem. C* 121 (11), 6141–6151. doi:10.1021/acs.jpcc.7b00196

Abghoui, Y., and Skúlason, E. (2017). Electrochemical synthesis of ammonia via Mars-van Krevelen mechanism on the (111) facets of group III–VII transition metal mononitrides. *Catal. Today* 286, 78–84. doi:10.1016/j.cattod.2016.06.009

Abghoui, Y., and Skúlason, E. (2017). Hydrogen evolution reaction catalyzed by transition-metal nitrides. *J. Phys. Chem. C* 121 (39), 24036–24045. doi:10.1021/acs.jpcc.7b06811

Abghoui, Y., and Skúlason, E. (2017). Onset potentials for different reaction mechanisms of nitrogen activation to ammonia on transition metal nitride electrocatalysts. *Catal. Today* 286, 69–77. doi:10.1016/j.cattod.2016.11.047

Abghoui, Y. (2022). Superiority of the (100) over the (111) facets of the nitrides for hydrogen evolution reaction. *Top. Catal.* 65 (1–4), 262–269. doi:10.1007/s11244-021-01474-5

Andersen, S. Z., Čolić, V., Yang, S., Schwalbe, J. A., Nielander, A. C., McEnaney, J. M., et al. (2019). A rigorous electrochemical ammonia synthesis protocol with quantitative isotope measurements. *Nature* 570 (7762), 504–508. doi:10.1038/s41586-019-1260-x

Azofra, L. M. (2022). Nitrogen reduction reaction (NRR) modelling: A case that illustrates the challenges of DFT studies in electrocatalysis. *Curr. Opin. Electrochem* 35, 101073. doi:10.1016/j.coelec.2022.101073

Blöchl, P. E. (1994). Projector augmented-wave method. *Phys. Rev. B* 50 (24), 17953–17979. doi:10.1103/PhysRevB.50.17953

Chanda, D., Xing, R., Xu, T., Liu, Q., Luo, Y., Liu, S., et al. (2021). Electrochemical nitrogen reduction: Recent progress and prospects. *Chem. Commun.* 57 (60), 7335–7349. doi:10.1039/D1CC01451J

Chen, Q., Zhang, X., Jin, Y., Zhou, X., Yang, Z., and Nie, H. (2020). An overview on noble metal (group VIII)-based heterogeneous electrocatalysts for nitrogen reduction reaction. *Chem – Asian J* 15 (24), 4131–4152. doi:10.1002/asia.202000969

Chen, S., Liu, X., Xiong, J., Mi, L., Song, X-Z., and Li, Y. (2022). Defect and interface engineering in metal sulfide catalysts for the electrocatalytic nitrogen reduction reaction: A review. *J. Mater Chem. A [Internet* 10 (13), 6927–6949. doi:10.1039/D2TA00070A

Choi, C., Gu, G. H., Noh, J., Park, H. S., and Jung, Y. (2021). Understanding potential-dependent competition between electrocatalytic dinitrogen and proton reduction reactions. *Nat. Commun.* 12 (1), 4353. doi:10.1038/s41467-021-24539-1

Choi, J., Suryanto, B. H. R., Wang, D., Du, H-L., Hodgetts, R. Y., Ferrero Vallana, F. M., et al. (2020). Identification and elimination of false positives in electrochemical nitrogen reduction studies. *Nat. Commun.* 11 (1), 5546. doi:10.1038/s41467-020-19130-z

Cui, X., Tang, C., and Zhang, Q. (2018). A review of electrocatalytic reduction of dinitrogen to ammonia under ambient conditions. *Adv. Energy Mater* 8 (22), 1800369. doi:10.1002/aenm.201800369

Cui, Z., Zu, C., Zhou, W., Manthiram, A., and Goodenough, J. B. (2016). Mesoporous titanium nitride-enabled highly stable lithium-sulfur batteries. *Adv. Mater* 28 (32), 6926–6931. doi:10.1002/adma.201601382

Dražević, E., and Skúlason, E. (2020). Are there any overlooked catalysts for electrochemical $NH_3$ synthesis—new insights from analysis of thermochemical data. *iScience* 23 (12), 101803. doi:10.1016/j.isci.2020.101803

Du, L., Xing, L., Zhang, G., Liu, X., Rawach, D., and Sun, S. (2021). Engineering of electrocatalyst/electrolyte interface for ambient ammonia synthesis. *SusMat* 1 (2), 150–173. doi:10.1002/sus2.7

Duan, G., Chen, Y., Tang, Y., Gasem, K. A. M., Wan, P., Ding, D., et al. (2020). Advances in electrocatalytic ammonia synthesis under mild conditions. *Prog. Energy Combust. Sci.* 81, 100860. doi:10.1016/j.pecs.2020.100860

Fu, W., Wang, K., Lv, X., Fu, H., Dong, X., Chen, L., et al. (2018). Palladium nanoparticles assembled on titanium nitride for enhanced electrochemical hydrodechlorination of 2, 4-dichlorophenol in water. *Chin. J. Catal.* 39 (4), 693–700. doi:10.1016/s1872-2067(17)62937-1

Fuller, J., An, Q., Fortunelli, A., and Goddard, W. A. (2022). Reaction mechanisms, kinetics, and improved catalysts for ammonia synthesis from hierarchical high throughput catalyst design. *Acc. Chem. Res.* 55 (8), 1124–1134. doi:10.1021/acs.accounts.1c00789

Garden, A. L., Abghoui, Y., and Skúlason, E. (2018). "Applications of transition metal nitrides as electrocatalysts," in *Alternative catalytic materials: Carbides, nitrides, phosphides and amorphous boron alloys*. Editors J. S. J. Hargreaves and R. S. L. AndrewMcFarlane (London: Royal society of chemistry), 133–163. Available at: https://pubs.rsc.org/en/content/ebook/978-1-78262-919-1.

Giddey, S., Badwal, S. P. S., Munnings, C., and Dolan, M. (2017). Ammonia as a renewable energy transportation media. *ACS Sustain Chem. Eng. [Internet]* 5 (11), 10231–10239. doi:10.1021/acssuschemeng.7b02219

Grimme, S., Antony, J., Ehrlich, S., and Krieg, H. (2010). A consistent and accurate *ab initio* parametrization of density functional dispersion correction (DFT-D) for the 94 elements H-Pu. *J. Chem. Phys.* 132 (15), 154104. doi:10.1063/1.3382344

Gu, G. H., Choi, C., Lee, Y., Situmorang, A. B., Noh, J., Kim, Y., et al. (2020). Progress in computational and machine-learning methods for heterogeneous small-molecule activation. *Adv. Mater [Internet]* 32 (35), 1907865. doi:10.1002/adma.201907865

Gudmundsson, M., Ellingsson, V., Skúlason, E., and Abghoui, Y. (2022). Optimizing nitrogen reduction reaction on nitrides: A computational study on crystallographic orientation. *Top. Catal.* 65 (1–4), 252–261. doi:10.1007/s11244-021-01485-2

Hammer, B., Hansen, L. B., and Nørskov, J. K. (1999). Improved adsorption energetics within density-functional theory using revised Perdew-Burke-Ernzerhof functionals. *Phys. Rev. B - Condens Matter Mater Phys.* 59, 7413–7421. doi:10.1103/PhysRevB.59.7413

Hanifpour, F., Canales, C. P., Fridriksson, E. G., Sveinbjörnsson, A., Tryggvason, T. K., Lewin, E., et al. (2022). Investigation into the mechanism of electrochemical nitrogen reduction reaction to ammonia using niobium oxynitride thin-film catalysts. *Electrochim Acta* 403, 139551. doi:10.1016/j.electacta.2021.139551

Hanifpour, F., Canales, C. P., Fridriksson, E. G., Sveinbjörnsson, A., Tryggvason, T. K., Yang, J., et al. (2022). Operando quantification of ammonia produced from computationally-derived transition metal nitride electro-catalysts. *J. Catal.* 413, 956–967. doi:10.1016/j.jcat.2022.07.030

Hanifpour, F., Sveinbjörnsson, A., Canales, C. P., Skúlason, E., and Flosadóttir, H. D. (2020). Preparation of nafion membranes for reproducible ammonia quantification in nitrogen reduction reaction experiments. *Angew. Chem.* 132 (51), 23138–23142. doi:10.1002/ange.202007998

Henkelman, G., and Jónsson, H. (2000). Improved tangent estimate in the nudged elastic band method for finding minimum energy paths and saddle points. *J. Chem. Phys.* 113 (22), 9978–9985. doi:10.1063/1.1323224

Hlynsson, V. F., Skúlason, E., and Garden, A. L. (2014). A systematic, first-principles study of the structural preference and magnetic properties of mononitrides of the d-block metals. *J. Alloys Compd.* 603, 172–179. doi:10.1016/j.jallcom.2014.02.153

Holmberg, K., and Erdemir, A. (2019). The impact of tribology on energy use and $CO_2$ emission globally and in combustion engine and electric cars. *Tribol. Int.* 135, 389–396. doi:10.1016/j.triboint.2019.03.024

Höskuldsson, Á. B., Tayyebi, E., and Skúlason, E. (2021). Computational examination of the kinetics of electrochemical nitrogen reduction and hydrogen evolution on a tungsten electrode. *J. Catal.* 404, 362–370. doi:10.1016/j.jcat.2021.10.017

Hossain, A. K., and Davies, P. A. (2013). Pyrolysis liquids and gases as alternative fuels in internal combustion engines – a review. *Renew. Sustain. Energy Rev.* 21, 165–189. doi:10.1016/j.rser.2012.12.031

Inumaru, K., Misono, M., and Okuhara, T. (1997). Structure and catalysis of vanadium oxide overlayers on oxide supports. *Appl. Catal. A Gen. [Internet* 149 (1), 133–149. doi:10.1016/s0926-860x(96)00254-2

Kelly, T. G., and Chen, J. G. (2012). Metal overlayer on metal carbide substrate: Unique bimetallic properties for catalysis and electrocatalysis. *Chem. Soc. Rev.* 41 (24), 8021. doi:10.1039/C2CS35165J

Kresse, G., and Furthmüller, J. (1996). Efficiency of *ab-initio* total energy calculations for metals and semiconductors using a plane-wave basis set. *Comput. Mater Sci.* 6 (1), 15–50. doi:10.1016/0927-0256(96)00008-0

Lai, Q., Zhang, C., and Holles, J. H. (2017). Mo@Pt overlayers as efficient catalysts for hydrodeoxygenation of guaiacol and anisole. *Catal. Sci. Technol.* 7 (15), 3220–3233. doi:10.1039/C7CY00565B

Lan, R., Irvine, J. T. S., and Tao, S. (2012). Ammonia and related chemicals as potential indirect hydrogen storage materials. *Int. J. Hydrogen Energy* 37 (2), 1482–1494. doi:10.1016/j.ijhydene.2011.10.004

Li, S., Zhou, Y., Li, K., Saccoccio, M., Sažinas, R., Andersen, S. Z., et al. (2022). Electrosynthesis of ammonia with high selectivity and high rates via engineering of the solid-electrolyte interphase. *Joule* 6 (9), 2083–2101. doi:10.1016/j.joule.2022.07.009

Li, X., Wei, J., Li, Q., Zheng, S., Xu, Y., Du, P., et al. (2018). Nitrogen-doped cobalt oxide nanostructures derived from cobalt-alanine complexes for high-performance oxygen evolution reactions. *Adv. Funct. Mater* 28 (23), 1800886. doi:10.1002/adfm.201800886

Li, Y., Zhang, Q., Mei, Z., Li, S., Luo, W., Pan, F., et al. (2021). Recent advances and perspective on electrochemical ammonia synthesis under ambient conditions. *Small Methods* 5 (11), 2100460. doi:10.1002/smtd.202100460

Liao, X., Lu, R., Xia, L., Liu, Q., Wang, H., Zhao, K., et al. (2022). Density functional theory for electrocatalysis. *ENERGY Environ. Mater [Internet]* 5 (1), 157–185. doi:10.1002/eem2.12204

Lide, D. R. E. (2004). *CRC handbook of chemistry and physics*, 85. Boca Raton: CRC Press.

Liu, A., Yang, Y., Ren, X., Zhao, Q., Gao, M., Guan, W., et al. (2020). Current progress of electrocatalysts for ammonia synthesis through electrochemical nitrogen reduction under ambient conditions. *ChemSusChem* 13 (15), 3766–3788. doi:10.1002/cssc.202000487

Loiseau, E., Saikku, L., Antikainen, R., Droste, N., Hansjürgens, B., Pitkänen, K., et al. (2016). Green economy and related concepts: An overview. *J. Clean. Prod.* 139, 361–371. doi:10.1016/j.jclepro.2016.08.024

Ma, L., Zhu, G., Wang, D., Chen, H., Lv, Y., Zhang, Y., et al. (2020). Emerging metal single atoms in electrocatalysts and batteries. *Adv. Funct. Mater* 30 (42), 2003870. doi:10.1002/adfm.202003870

MacFarlane, D. R., Cherepanov, P. V., Choi, J., Suryanto, B. H. R., Hodgetts, R. Y., Bakker, J. M., et al. (2020). A roadmap to the ammonia economy. *Joule* 4 (6), 1186–1205. doi:10.1016/j.joule.2020.04.004

MacLaughlin, C. (2019). Role for standardization in electrocatalytic ammonia synthesis: A conversation with leo Liu, lauren greenlee, and douglas MacFarlane. *ACS Energy Lett.* 4 (6), 1432–1436. doi:10.1021/acsenergylett.9b01123

Manjunatha, R., Karajić, A., Liu, M., Zhai, Z., Dong, L., Yan, W., et al. (2020). A review of composite/hybrid electrocatalysts and photocatalysts for nitrogen reduction reactions: Advanced materials, mechanisms, challenges and perspectives. *Electrochem. Energ. Rev.* 3 (3), 506–540. doi:10.1007/s41918-020-00069-0

Michalsky, R., Avram, A. M., Peterson, B. A., Pfromm, P. H., and Peterson, A. A. (2015). Chemical looping of metal nitride catalysts: Low-pressure ammonia synthesis for energy storage. *Chem. Sci.* 6 (7), 3965–3974. doi:10.1039/c5sc00789e

Michalsky, R., Pfromm, P. H., and Steinfeld, A. (2015). Rational design of metal nitride redox materials for solar-driven ammonia synthesis. *Interface Focus* 5 (3), 1–10. doi:10.1098/rsfs.2014.0084

Pretty, J. (2013). The consumption of a finite planet: Well-being, convergence, divergence and the nascent green economy. *Environ. Resour. Econ.* 55 (4), 475–499. doi:10.1007/s10640-013-9680-9

Qing, G., Ghazfar, R., Jackowski, S. T., Habibzadeh, F., Ashtiani, M. M., Chen, C-P., et al. (2020). Recent advances and challenges of electrocatalytic $N_2$ reduction to ammonia. *Chem. Rev.* 120 (12), 5437–5516. doi:10.1021/acs.chemrev.9b00659

Rehman, F., Delowar Hossain, M., Tyagi, A., Lu, D., Yuan, B., and Luo, Z. (2021). Engineering electrocatalyst for low-temperature $N_2$ reduction to ammonia. *Mater. Today* 44, 136–167. doi:10.1016/j.mattod.2020.09.006

Shen, H., Choi, C., Masa, J., Li, X., Qiu, J., Jung, Y., et al. (2021). Electrochemical ammonia synthesis: Mechanistic understanding and catalyst design. *Chem* 7 (7), 1708–1754. doi:10.1016/j.chempr.2021.01.009

Singh, A. R., Rohr, B. A., Statt, M. J., Schwalbe, J. A., Cargnello, M., and Nørskov, J. K. (2019). Strategies toward selective electrochemical ammonia synthesis. *ACS Catal.* 9 (9), 8316–8324. doi:10.1021/acscatal.9b02245

Tayyebi, E., Abghoui, Y., and Skúlason, E. (2019). Elucidating the mechanism of electrochemical $N_2$ reduction at the Ru(0001) electrode. *ACS Catal.* 9 (12), 11137–11145. doi:10.1021/acscatal.9b03903

Wan, H., Bagger, A., and Rossmeisl, J. (2022). Improved electrocatalytic selectivity and activity for ammonia synthesis on diporphyrin catalysts. *J. Phys. Chem. C* 126 (39), 16636–16642. doi:10.1021/acs.jpcc.2c05646

Wang, K., Smith, D., and Zheng, Y. (2018). Electron-driven heterogeneous catalytic synthesis of ammonia: Current states and perspective. *Carbon Resour. Convers.* 1 (1), 2–31. doi:10.1016/j.crcon.2018.06.004

Yang, B., Ding, W., Zhang, H., and Zhang, S. (2021). Recent progress in electrochemical synthesis of ammonia from nitrogen: Strategies to improve the catalytic activity and selectivity. *Energy Environ. Sci.* 14 (2), 672–687. doi:10.1039/D0EE02263B

Yao, D., Tang, C., Wang, P., Cheng, H., Jin, H., Ding, L-X., et al. (2022). Electrocatalytic green ammonia production beyond ambient aqueous nitrogen reduction. *Chem. Eng. Sci.* 257, 117735. doi:10.1016/j.ces.2022.117735

Zeinalipour-Yazdi, C. D., Hargreaves, J. S. J., and Catlow, C. R. A. (2015). Nitrogen activation in a Mars-van Krevelen mechanism for ammonia synthesis on $Co_3Mo_3N$. *J. Phys. Chem. C* 119, 28368–28376. doi:10.1021/acs.jpcc.5b06811

Zhang, L., Hou, S., Wang, T., Liu, S., Gao, X., Wang, C., et al. (2022). Recent advances in application of graphitic carbon nitride-based catalysts for photocatalytic nitrogen fixation. *Small* 18, 2202252. doi:10.1002/smll.202202252

Zhou, D., Guo, X., Zhang, Q., Shi, Y., Zhang, H., Yu, C., et al. (2022). Nickel-based materials for advanced rechargeable batteries. *Adv. Funct. Mater* 32 (12), 2107928. doi:10.1002/adfm.202107928